Please cite this article in press as: Tam et al., Genome-edited safe and immune-evasive human pluripotent cells: Potential solution for allogeneic therapies, Stem Cell Reports (2026), https://doi.org/10.1016/j.stemcr.2026.102850

STEM CELL REPORTS
Article
ISSCR
OPEN ACCESS

Genome-edited safe and immune-evasive human pluripotent cells: Potential solution for allogeneic therapies

Vivian Tam,[1,6] Nicole Ching Man Wong,[1,6] Andrew Chung Hin Poon,[1] Mengxia Zhu,[1] Ting Mei,[1] Janette Kwok,[2] Patrick Chu,[2] Eric D. Jong,[3] Jean Kit Tang,[3,4] Andras Nagy,[3,5,*] and Danny Chan[1,7,*]
[1]School of Biomedical Sciences, Li Ka Shing Faculty of Medicine, The University of Hong Kong, Hong Kong SAR, China
[2]Division of Transplantation & Immunogenetics, Department of Pathology, Queen Mary Hospital, Hong Kong SAR, China
[3]Lunenfeld-Tanenbaum Research Institute, Sinai Health System, Toronto, ON, Canada
[4]Department of Physiology, University of Toronto, Toronto, ON, Canada
[5]Department of Obstetrics & Gynaecology and Institute of Medical Science, University of Toronto, Toronto, ON, Canada
[6]These authors contributed equally
[7]Lead contact
*Correspondence: nagy@lunenfeld.ca (A.N.), chand@hku.hk (D.C.)
https://doi.org/10.1016/j.stemcr.2026.102850

SUMMARY

We used an embryonic stem cell line (H1) engineered for immune-evading properties to avoid rejection ("AlloAccept") and equipped with a "SafeCell" (SC) kill-switch to eliminate aberrantly proliferating cells. Utilizing a humanized immune system mouse model, we demonstrated the successful generation of allogeneic tissues from SafeCell-AlloAccept (SC-AlloAccept) cells in immunocompetent humanized mice in the immune-active subcutaneous region. These cells formed various tissue types, and their growth can be controlled with prodrug ganciclovir to activate the kill switch, which eliminated proliferating cells and rendered the remaining tissue dormant. Strikingly, SC-AlloAccept-derived grafts survived for 5 months, underscoring their potential for long-term engraftment. Importantly, neither prior rejection of immunogenic parental H1 cells (sensitization) nor the presence of immune-evasive H1-derived tissue (potential immunocompromising) affected the immune response to a subsequent second transplant. This study validated the utility of SC-AlloAccept human cells in transplantation and enhanced the safety and efficacy of stem cell-based regenerative therapies.

INTRODUCTION

Cell therapies using pluripotent stem cells (PSCs) and tissue transplantation are promising modalities to revolutionize the treatments of diseases enhancing patient outcomes. Reprograming somatic cells into PSCs can generate patient-specific autologous therapeutic cells, recognized as self by the immune system, the manufacturing process remains limited by high costs and prolonged timelines at scale.

The broad and efficient clinical adoption of cell therapies requires solving two key challenges: (1) developing immune-evasive allogeneic cells that can be accepted by patients and (2) ensuring the safety of these immune-evasive and *in vitro* expanded therapeutic cells (Harding et al., 2020). Genome editing approaches have developed to address the first challenge (Hotta et al., 2024) by manipulating the major histocompatibility complex (MHC)/human leukocyte antigen (HLA) genes. An alternative is to engineer donor cells to express a set of immune-modulating transgenes (*PD-L1*, *CD200*, *CD47*, *FASL*, *SERPINB9*, *CCL21*, *MFGE8*, and *H2-M3*) without altering the MHC/HLA genes, thereby "cloaking" them from allogeneic rejection by inhibiting innate and adaptive immune responses, including those mediated by DCs, T cells, NK cells, and monocytes/macrophages (Harding et al., 2024).

When these transgenic mouse embryonic stem cells (ESCs) were injected into allogeneic (MHC-mismatched) immunocompetent mice, they were not rejected and formed growing tissues, unlike non-transgenic cells. This genomic modification in the cells is termed "AlloAccept" (Allogeneic Cell Accepted). The cells were also equipped with the SafeCell (SC) genome edit (Liang et al., 2018), providing a safety switch that enables selective elimination of transplanted cells with potential oncogenic proliferation. Due to the functional conservation of the 8 immune modulatory genes between mouse and human (Harding et al., 2024), H1 human ESCs and their derivatives expressing the orthologous genes can effectively suppress adaptive and innate immune activation *in vitro*, and co-culture with human peripheral blood mononuclear cells (PBMCs) (Harding et al., 2024; Pavan et al., 2025). While the *in vitro* assays provide insights into immune responses to the human SC-AlloAccept cells, it is crucial to assess their behavior *in vivo*. A recent study utilizing a humanized mouse model of Parkinson's disease reported successful brain engraftment of neurons differentiated from the SC-AlloAccept (previously named H1-FS-8IM; Pavan et al., 2025) cells. Compared with control grafts, SC-AlloAccept neural transplants formed larger grafts with more neurons and fewer local inflammatory cells. Mice receiving SC-AlloAccept cells also had reduced levels of T cells and proinflammatory cytokines, indicating minimal immune activation (Pavan et al., 2025).

While there was successful immune evasion of SC-AlloAccept cells in the brain, the CNS is a sequestered,

Please cite this article in press as: Tam et al., Genome-edited safe and immune-evasive human pluripotent cells: Potential solution for allogeneic therapies, Stem Cell Reports (2026), https://doi.org/10.1016/j.stemcr.2026.102850

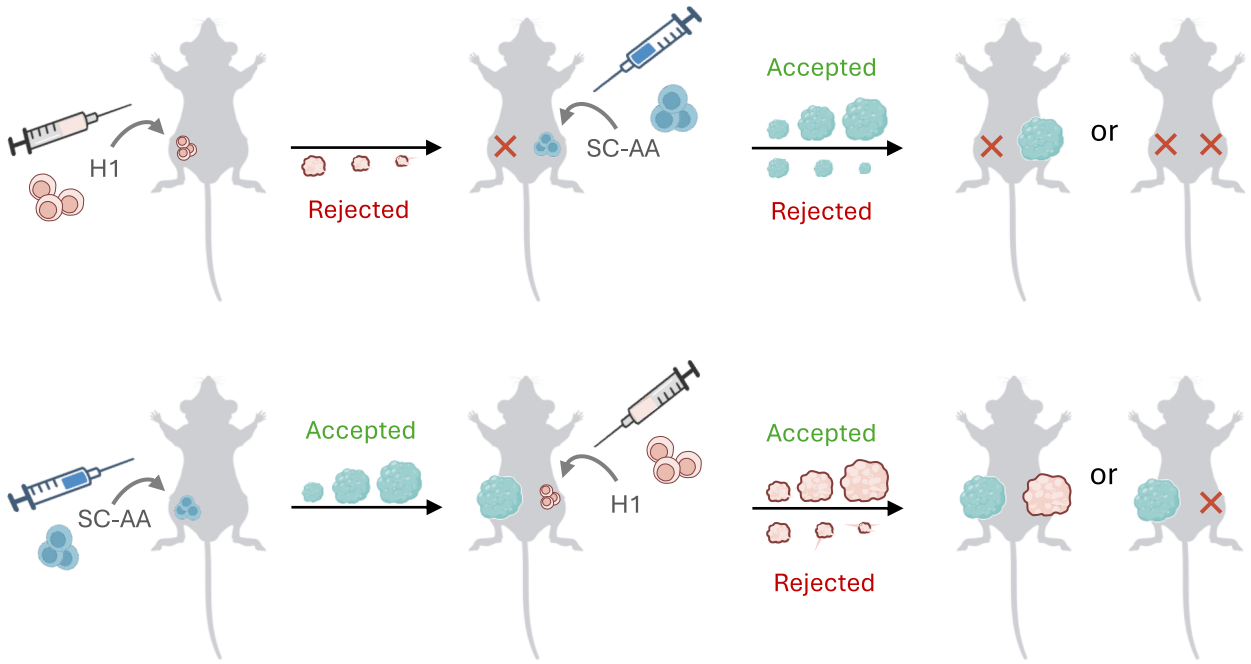

Figure 1. Schematic of experimental hypotheses

Top: following rejection of allogeneic H1 hESCs by a humanized immune system, subsequent transplantation of cloaked SafeCell-AlloAccept (SC-AA) cells may lead either to rejection (due to prior sensitization) or to long-term engraftment (if immune protection is sufficient). Bottom: if SC-AA cells are transplanted first, a later H1 graft may either be accepted (via systemic immune modulation by established SC-AA tissue) or rejected (if the immune system remains unaffected).

immune-privileged site that supports graft acceptance, and is minimally immune-active. Consequently, to prove the universal efficacy of SC-AlloAccept cells, we validated their survival in highly immune-active environments—in the subcutaneous space—using a humanized immune system model that provides a more rigorous challenge than the brain.

We further showed tissue growth could be regulated by activation of the SC kill switch with the prodrug ganciclovir (GCV). In addition, we assessed whether prior sensitizing of the host immune system by rejection of parental H1 cells influenced the acceptance of SC-AlloAccept cells, and vice-versa, and whether established SC-AlloAccept cell-derived grafts compromised the rejection of parental H1 cells (Figure 1). This study highlights that SC-AlloAccept tissues can survive long-term in allogeneic humanized mice, underscoring the potential for universal allogeneic tissue transplantation.

RESULTS

AlloAccept cells evade immune cell responses *in vitro*

Due to the complexity and physiological limitations of studying human immune reactions in humanized mice, we first examined how specific cell types interact with SC-AlloAccept ESCs *in vitro*, and to confirm immune-evasive properties aligning with previous findings in retinal pigmented epithelium (RPE) derived from the same SC-AlloAccept ESC line (Harding et al., 2024). First, we co-cultured SC-AlloAccept ESCs with human Jurkat T cells (Abraham and Weiss, 2004) to evaluate helper T cell activation, and with NK92MI cells (Tam et al., 1999) to model the innate immune system response.

Co-culturing SC-AlloAccept cells with Jurkat T cells for one day led to upregulation of the T cell activation marker CD69, but its levels were lower than in T cells exposed to parental H1 cells or the positive control (Figure S1A), indicating a dampened T cell response. Similarly, SC-AlloAccept cells significantly decreased NK92MI cell expression of proinflammatory markers *IFNγ*, *TNFα*, and *GZMB* compared with H1 cells and the positive control (Figure S1B), indicating that the NK92MI cells were not effectively activated, consistent with previous findings, with the expected immune-modulatory function (Harding et al., 2024; Pavan et al., 2025), including PBMC-derived NK cells.

To study the immune interactions of SC-AlloAccept cells within a normal human blood context, we co-cultured them with allogeneic human PBMCs. Assessment by flow

cytometry showed activation of DCs (HLA-DR$^+$ of CD11C$^+$ cells), CD4$^+$ T cells (CD4$^+$CD25$^+$ cells), and monocytes (HLA-DR$^+$ of CD16$^+$ cells). The SC-AlloAccept cells significantly reduced the activation levels of DCs (19.5% vs. 49.7%), T cells (13.0% vs. 27.5%), and monocytes (8.9% vs. 62.1%) compared to uncloaked cells (Figures S1C–S1E). Previous CyTOF analyses of co-cultured CD8$^+$ T cells and SC-AlloAccept-derived RPE reduced the numbers of both memory and effector CD8$^+$ T cells (Harding et al., 2024), and were not further analyzed in this study. In all, our findings support hypo-immunogenicity of the SC-AlloAccept cells.

Further, enzyme-linked immunosorbent assay (ELISA) assessment of PBMC secretion of proinflammatory cytokines IFNγ and TNFα, markers that correlate with T cell activation (Qudus et al., 2023; Szabo et al., 2003) were reduced when co-cultured with SC-AlloAccept cells compared to uncloaked cells (Figure S1F), again supporting hypoimmunogenicity of the SC-AlloAccept cells. In all, the *in vitro* suggests the human SC-AlloAccept cells would not be rejected by mice with a humanized immune system.

Source, time point status, and HLA typing of the humanized mice and SafeCell-AlloAccept human ESCs

Ten humanized immune system mice were purchased from GemPharmatech (see "methods") (Figures S2A and S2B). Compared to typical human levels (Jentsch-Ullrich et al., 2005), these mice had less T cells and monocytes, and more B cells. Humanization status was monitored by flow cytometry on the peripheral blood at available time points, and from bone marrow aspirates at the experimental endpoint (Figure S2C). The extent of humanization, as measured by the proportion of human CD45$^+$ cells was decreased from the initial average of 40%–27% by the endpoint of the experiments. The level of B cells was significantly reduced, from 87% to 5.9%; in contrast, the proportion of T cells was significantly increased from 0.23% to 17.31%, whereas monocytes were slightly decreased from 7.29% to 4.11% at the endpoint (Figure S2C). These changes in cell proportions aligned with previous studies using the humanized mice model (Ménoret et al., 2024; Yahata et al., 2002; Yu et al., 2024).

The probability of a full HLA match among the six key loci (HLA-A, -C, -B, -DRB1, -DQB1, and -DPB1) between the human hematopoietic donor cells the H1-derived SC-AlloAccept cells is ∼1 in 100,000 (Mahdi, 2019), making a perfect match highly unlikely. Consistent with this, HLA typing and confirmed complete HLA mismatch at all class I and class II loci, including HLA-A, -C, -B, -DRB1, -DQB1, and -DPB1 (Figure S2D) ensuring that engraftment in humanized mice reflects SC-AlloAccept immune evasion.

AlloAccept cell-generated tissues are accepted in humanized mice, and growth is controlled by the SC system

Undifferentiated ESCs exhibit low immunogenicity and become more immunogenic upon differentiation due to upregulated MHC/HLA expression (Bifari et al., 2010; Drukker et al., 2002). To enhance the immunogenicity before transplantation, SC-AlloAccept and control cells were differentiated toward mesendoderm using our established protocol (Figure S3A) (Warin et al., 2024). Although differentiation was toward the mesendoderm, populations of progenitors from lateral/paraxial mesoderm and axial progenitors, as well as minor populations resembling neurectoderm, neuromesodermal progenitors, and endoderm were present (Warin et al., 2024).

Differentiated H1 SC-AlloAccept and control cells were transplanted subcutaneously into two groups of humanized mice, SC-AlloAccept-(1–5) and H1-(1–5) (Figure 2A). Mice were monitored for body weight and peripheral blood content by flow cytometry for indications of graft versus host disease (GvHD) resulting from humanization. Transplants were monitored for growth by bioluminescence imaging (BLI), palpation, and caliper-based volume measurements.

One H1 recipient (H1-5) died on day 3 from anesthesia complications, but remaining H1 mice were followed for >140 days (Figure 2Bi). These mice showed a modest decline in body weight (Figure 2Bii). From day 46 onwards, graft measurements indicated no increase in H1 transplant volume (Figure 2Biii). BLI revealed reduced luminescence of injected cells after day 0, a continual decrease in luminescence or persistence with no observable tissue growth (Figure 2Biv, v). In two of the mice, a small and likely scar tissue mass was noted. These findings are consistent with H1 cells being rejected by the functional humanized immune system. In contrast, H1 SC-AlloAccept cell transplants rapidly formed enlarging palpable subcutaneous tissue in all five mice (Figure 2Ci to 1Ciii), indicating protection from allogeneic rejection.

When the transplant reached ∼500 mm^3, we activated the SC system by administering GCV to the animals for 7–14 days, which halted further tissue growth and enabled assessment of long-term persistence of the allogeneic tissues (Figure 2Ciii). Across the experimental period, body weight remained stable in four of five mice (Figure 2Cii), consistent with the absence of GvHD. As GCV ablates proliferating cells (Liang et al., 2018), a reduction and subsequent stabilization of graft size at ∼100–250 mm^3 was anticipated (Figures 1Ciii and S3B). The BLI signals mirrored the tissue volume changes (Figure 2Civ, v). The stabilized tissues persisted with similar volumes for 5 months, demonstrating long-term acceptance of the H1 SC-AlloAccept cells in humanized allogeneic recipient.

Please cite this article in press as: Tam et al., Genome-edited safe and immune-evasive human pluripotent cells: Potential solution for allogeneic therapies, Stem Cell Reports (2026), https://doi.org/10.1016/j.stemcr.2026.102850

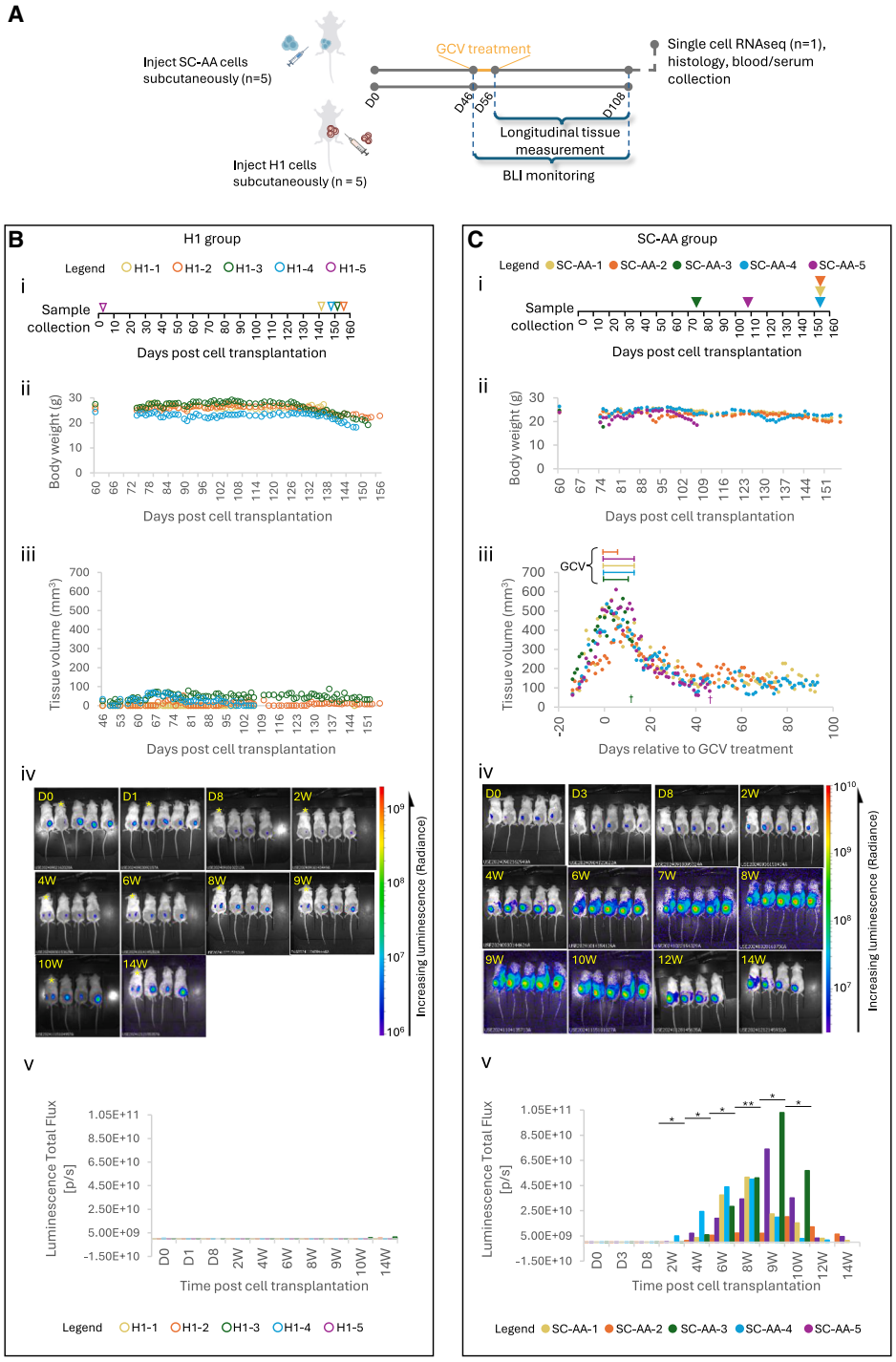

Figure 2. SC-AlloAccept-derived tissues were not rejected in allogeneic humanized mice

(A) Schematic of study design. SC-AlloAccept (SC-AA) or H1 cells transfected with luciferase were injected into humanized mice and growth monitored over time.

(B and C) Time points harvested (Bi and Ci), body weight of mice (Bii and Cii), and tissue growth measurements (Biii and Ciii, † and † denote end time point for the respective mice). When grafts reached ~500 mm^3, mice received GCV for up to 2 weeks until tissue size stabilized. Day 0 was defined as start of GCV treatment to align tissue-size dynamics across animals (Ciii). Tissue growth was also monitored by BLI (Biv and Civ). Luminescence of tissue growth was quantified (Bv and Cv, $n = 3–5$ biological replicates). Significance relative to D0: $*p < 0.05$, $**p < 0.01$. *One H1 group mouse was injected on both sides with H1 cells.

Please cite this article in press as: Tam et al., Genome-edited safe and immune-evasive human pluripotent cells: Potential solution for allogeneic therapies, Stem Cell Reports (2026), https://doi.org/10.1016/j.stemcr.2026.102850

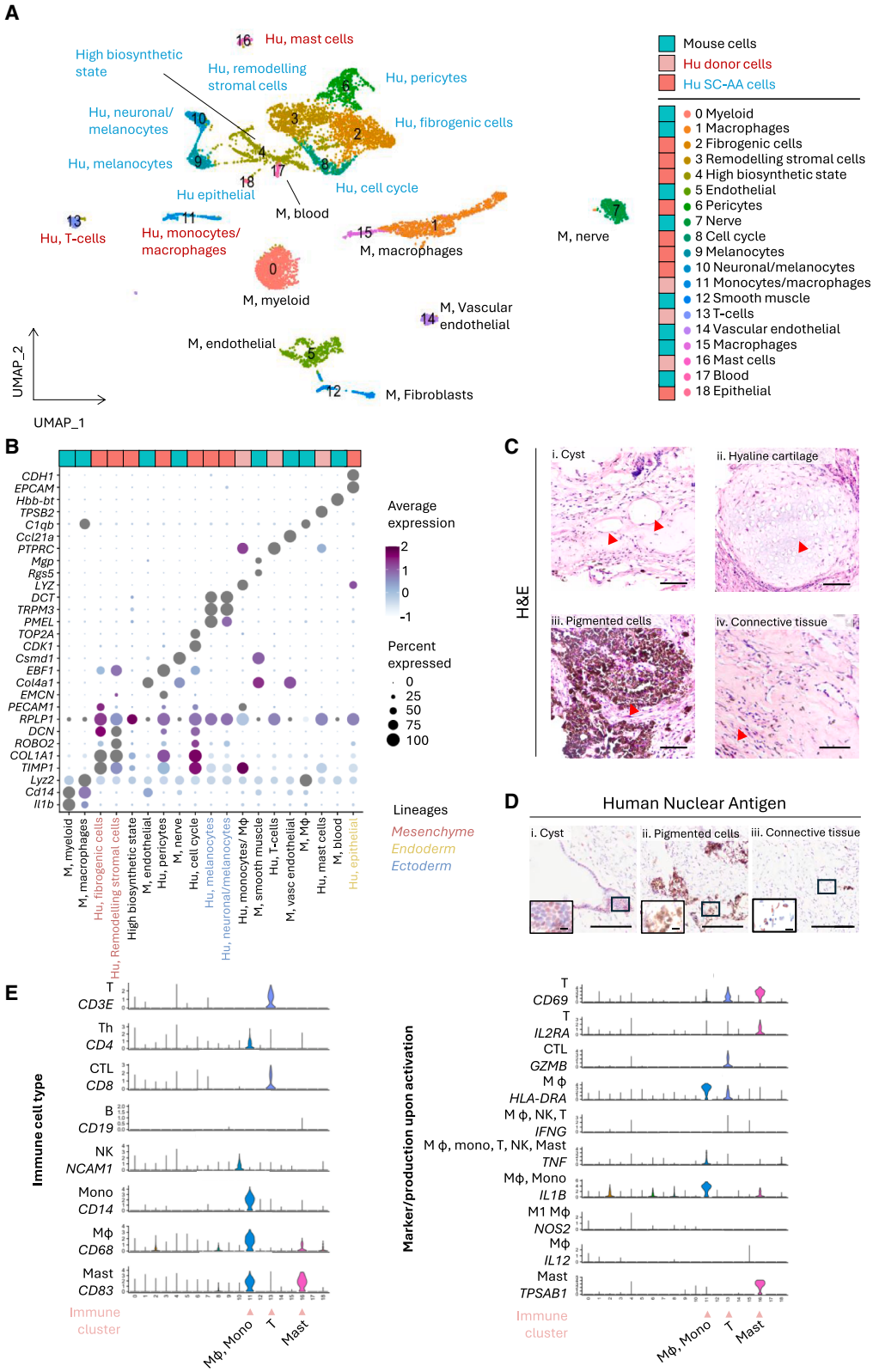

(legend on next page)

Please cite this article in press as: Tam et al., Genome-edited safe and immune-evasive human pluripotent cells: Potential solution for allogeneic therapies, Stem Cell Reports (2026), https://doi.org/10.1016/j.stemcr.2026.102850

Tissues formed from SC-AlloAccept cells are well tolerated and integrate into the humanized immune system hosts

Two SC-AlloAccept recipients (SC-AA-3 and SC-AA-5) had to be euthanized due to weight loss on days 75 and 108 post-transplantation, respectively. For mouse SC-AA-5, this was 34 days after GCV treatment (Figure 2Ciii). The tissue was excised for histological examination and single-cell RNA sequencing (RNAseq) performed to determine the graft composition. Using 10X genomics, we identified distinct cell populations of mouse and human cell origins (Figure 3A). Host human (female) versus SC-AlloAccept (male) cells were further resolved by XIST and UTY expression, respectively (Figure S4A). The eight immuno-cloaking transgenes were expressed in the human SC-AlloAccept cells (Figure S4B), with overall patterns similar to a previous mesendoderm differentiation dataset (Warin et al., 2024) (Figure S4B), and previous reports of low HLA-G expression (Harding et al., 2024; Pavan et al., 2025).

In this transplant, we identified 19 distinct clusters (Figure 3A), eight were of mouse origin (clusters 0, 1, 5, 7, 12, 14, 15, and 17), eight from the human SC-AlloAccept cells (clusters 2, 3, 4, 6, 8, 9, 10, and 18), and three from the human blood cells of humanization origin (clusters 11, 13, and 16). These included a population of mast cells (cluster 16), T cells predominantly expressing $CD8^+$ with few $CD4^+$ T cells (cluster 13), and monocytes/macrophages (cluster 11). There were no B cell or NK cell clusters in the tissue.

Analysis of SC-AlloAccept-derived clusters revealed differentiated cells along all three germ cell lineages. Based on top gene markers (Figures 3B, S4C, and S4D), we identified mesodermal populations including fibrogenic cells (cluster 2), *EBF1*+ pericytes (cluster 6), and extracellular matrix (ECM) remodeling cells (cluster 3); endoderm lineage of *CDH1*-expressing epithelial cells, (Figures 3B and S4E); and ectoderm lineage cell types (*PMEL*+ melanocytes; Figure 3B). There were also cells expressing endothelial markers CD31 (*PECAM1*) and endomucin (*EMCN*) (Figures 3B and S4F), signifying that the SC-AlloAccept cells can contribute to potential capillary-like structures *in vivo*. Hematoxylin and eosin (H&E) staining showed cyst-like structures, pigmented cells, hyaline cartilage, and connective tissue (Figure 3C). Across different structures within the tissues, most cells were of human origin (HNA+, red stain) surrounded by HNA-negative mouse epithelium (Figure 3D).

Cells in cluster 4 of SC-AlloAccept origin expressed high levels of mitochondrial and ribosomal genes, indicating an active biosynthesis state, where subclustering identified melanocytes, fibrogenic, epithelial-mesenchymal transition (EMT), neuronal oxidative phosphorylation (OXPHOS), neuronal/axon, stromal/ECM remodeling, and mouse myeloid cells (Figure S4Gi). Cluster 8 was a population of cells in the cell cycle (Figure 3A). This suggests that, while these cells were not actively proliferating, due to stabilized tissue size from prior GCV treatment, they were likely arrested or paused at specific cell cycle checkpoints. Further subclustering showed the presence of neuronal, ECM/remodeling, and inflammatory fibrogenic cells within this cluster (Figure S4Gii).

Next, we assessed immune evasion by examining activation markers and proinflammatory cytokines in donor human immune cell clusters. In T cells, CD69 expression was low, with cytotoxic T lymphocytes expressing low levels of *GZMB*, but no activation marker *IL2RA* on $CD4^+$ T cells (Figure 3E). Macrophages showed increased *HLA-DRA* and *IL1B*, but no *IFNG*, *NOS2*, or *IL12*, consistent with minimal monocytes/macrophage activation (Figure 3E). In contrast, mast cells exhibited elevated expression of tryptase mediator *TPSAB1*, *CD69*, *IL2RA*, and low levels of *IL1B*, indicating they were activated with a modest inflammatory response (Figure 3E). Overall, SC-AlloAccept cells were well tolerated by the monocytes, macrophages, and T cells, with evidence of mast cell activation, that could either be proinflammatory or anti-inflammatory depending on the cytokine environment (Tsai et al., 2011).

Mouse-derived clusters corresponded to myeloid, endothelial, smooth muscle, macrophages, blood, nerve, and vascular cell types (Figures 3A and 3B), indicating mouse cells were well integrated within the graft. This host vasculature likely supplied oxygen and nutrients necessary for long-term SC-AlloAccept tissue survival and maintenance. Collectively, these how that SC-AlloAccept cells persisted post-GCV treatment with vascular support from the mouse cells and did not elicit an immune response leading to rejection in humanized allogeneic recipients.

Figure 3. Single-cell RNAseq and histology of SC-AlloAccept (SC-AA) tissues 108 days post-transplantation in humanized mice (SC-AA-5)

(A) UMAP plot showing dataset clustering and annotation.

(B) Dot plot showing marker expression across clusters.

(C) H&E staining showed presence cyst-like structures, hyaline cartilage, pigmented cells, and connective tissue.

(D) IHC for human nuclear antigen confirmed that the tissues are human cell-derived.

(E) Violin plots show immune cell and activation markers expression. Abbreviations: Mφ, macrophages; Mono, monocytes. Scale bars, 200 μm; inset 60x scale bars, 10 μm.

Please cite this article in press as: Tam et al., Genome-edited safe and immune-evasive human pluripotent cells: Potential solution for allogeneic therapies, Stem Cell Reports (2026), https://doi.org/10.1016/j.stemcr.2026.102850

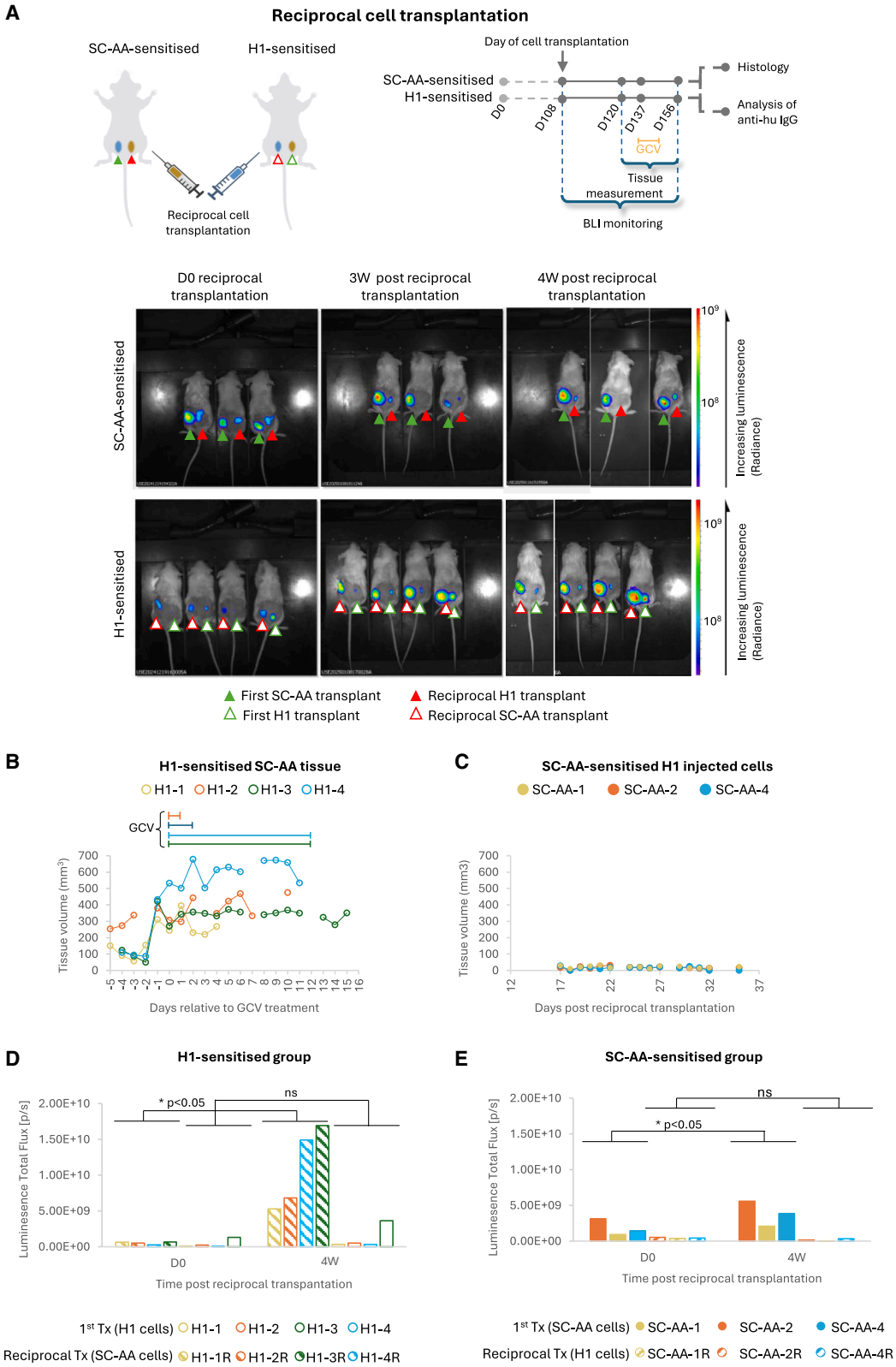

(legend on next page)

Prior allogeneic immune challenge does not alter the immunocompetence of the humanized mice

We reasoned mice which had rejected H1 cells would have a sensitized immune system. To test whether such sensitized hosts could accept SC-AlloAccept cells, we transplanted SC-AlloAccept cells into the contralateral flank of these animals. Conversely, to assess whether established SC-AlloAccept grafts altered the immune system's capacity to reject wild-type H1 cells, we performed a reciprocal transplantation of H1 cells into the opposite flank (Figure 4A). In sensitized recipients that had rejected H1 cells, SC-AlloAccept cells were nonetheless accepted and rapidly formed expanding grafts (Figures 4B and D). GCV administration effectively activated the SC system to control graft growth (Figure 4B). Therefore, the SC-AlloAccept system offers strong protection to allogeneic cells, even in hosts sensitized to the parental H1 line.

In the reverse experiment, H1 cells were transplanted into mice maintaining a stable subcutaneous tissue derived from SC-AlloAccept cells. Over the 35-day, the transplanted H1 cells did not form palpable tissues, indicating that the presence of AlloAccept tissue does not affect the systemic immune system's ability to reject wild-type H1 cells (Figure 4C). Importantly, sizes of existing SC-AlloAccept grafts remained stable even as the H1-derived second challenge cells were eliminated (Figure 4E), suggesting that the SC-AlloAccept cells continued to be protected despite the active rejection of the new H1 cell transplant.

SC-AlloAccept cells upheld survival and graft tissue integrity despite a prompted adaptive immune response

Graft rejection can occur via cellular mechanisms, mediated by $CD4^+$ helper T cells and/or $CD8^+$ cytotoxic T cells recognzing mismatched HLA, or via antibody-mediated rejection that drive inflammatory damage of the graft (Griffith et al., 2025; Harper et al., 2015). Since the SC-AlloAccept cells grew even in mice that had rejected parental H1 cells (as shown in SC-AlloAccept tissue, Figure 4), while typically this scenario would trigger an adaptive immune response, we next characterized immune infiltrates within accepted SC-AlloAccept tissues. We examined tissues in mice that were either sensitized with H1 cells or not (unexposed mice that have only been treated with SC-AlloAccept tissue) (Figure 5A).

We assess for $CD4^+$ T cell infiltration (Figures 5B and 5C), that were more abundant in the periphery of the tissue, particularly in mouse H1-2 (Figures 5B and 5C). Quantification showed significantly higher $CD4^+$ cells in the SC-AlloAccept tissue of H1-sensitized mice versus unsensitized mice (Figure 5D). In contrast, few $CD8^+$ cells were in the tissues (Figure S5A), suggesting a predominantly $CD4^+$ T cell response, or the $CD8^+$ T cells were eliminated from the tissue. Few $CD68^+$ macrophages were detected (Figures 5B and 5C). We identified $CD56^+$ cells (Figure S5B, left), however, scRNA-seq analysis of cluster 10 indicated a neuronal rather than NK-cell identity (Figure S5B, right).

In addition to cellular immunity, humoral immune responses play a significant role in graft rejection by targeting donor antigens. Using anti-human IgG antibodies, we detected robust human IgG deposition in SC-AlloAccept grafts of H1-sensitized mice (Figure 5E), but not in unsensitized mice (Figure 5F). To further verify that the signal was specifically from human IgG, we used FcX blocker on the SC-AlloAccept tissue of H1-sensitized mice (Figure S5C), which reduced the fluorescence signal and confirmed specificity for human IgG. Quantification of IgG signal normalized to DAPI, revealed higher levels in mouse H1-2 than in SC-AA-1 mouse (Figure 5G), indicating that H1-sensitization induced a human antibody response not seen in non-sensitized hosts.

In summary, immune cell infiltrates and anti-human antibodies within the SC-AlloAccept tissues did not prevent engraftment and growth of the AlloAccept cells, even in immune-active hosts. Moreover, the absence of significant cell death (Figure 5H) suggests a stable coexistence between the humanized immune system and the allogeneic SC-AlloAccept cells. This highlights the robust protection conferred by the AlloAccept system, enabling long-term graft survival despite potential immune challenges.

Figure 4. Reciprocal transplantation into the humanized mice

(A) Schematic and BLI of subcutaneous reciprocal transplants: H1-sensitized mice received SC-AlloAccept (SC-AA) cells, and SC-AA-sensitized mice received H1 cells.

(B) H1-sensitized SC-AA tissue volumes. When grafts reached ~500 mm^3, mice received GCV for up to 2 weeks until tissue size stabilized. Day 0 was defined as start of GCV treatment to align tissue-size dynamics across animals.

(C) Tissue volume measurements of H1 cells in SC-AA-sensitized mice showed no development of a palpable mass.

(D) Quantification in H1-sensitized mice showed significantly increased growth of SC-AA cells, but not of H1 cells from the first transplantation ($n = 4$ biological replicates).

(E) In SC-AA-sensitized mice, H1 cell growth was unchanged, while SC-AA cells from the first transplantation showed a small but significant increase ($n = 3$ biological replicates). Statistical significance relative to D0: $*p < 0.05$; ns, not significant.

Please cite this article in press as: Tam et al., Genome-edited safe and immune-evasive human pluripotent cells: Potential solution for allogeneic therapies, Stem Cell Reports (2026), https://doi.org/10.1016/j.stemcr.2026.102850

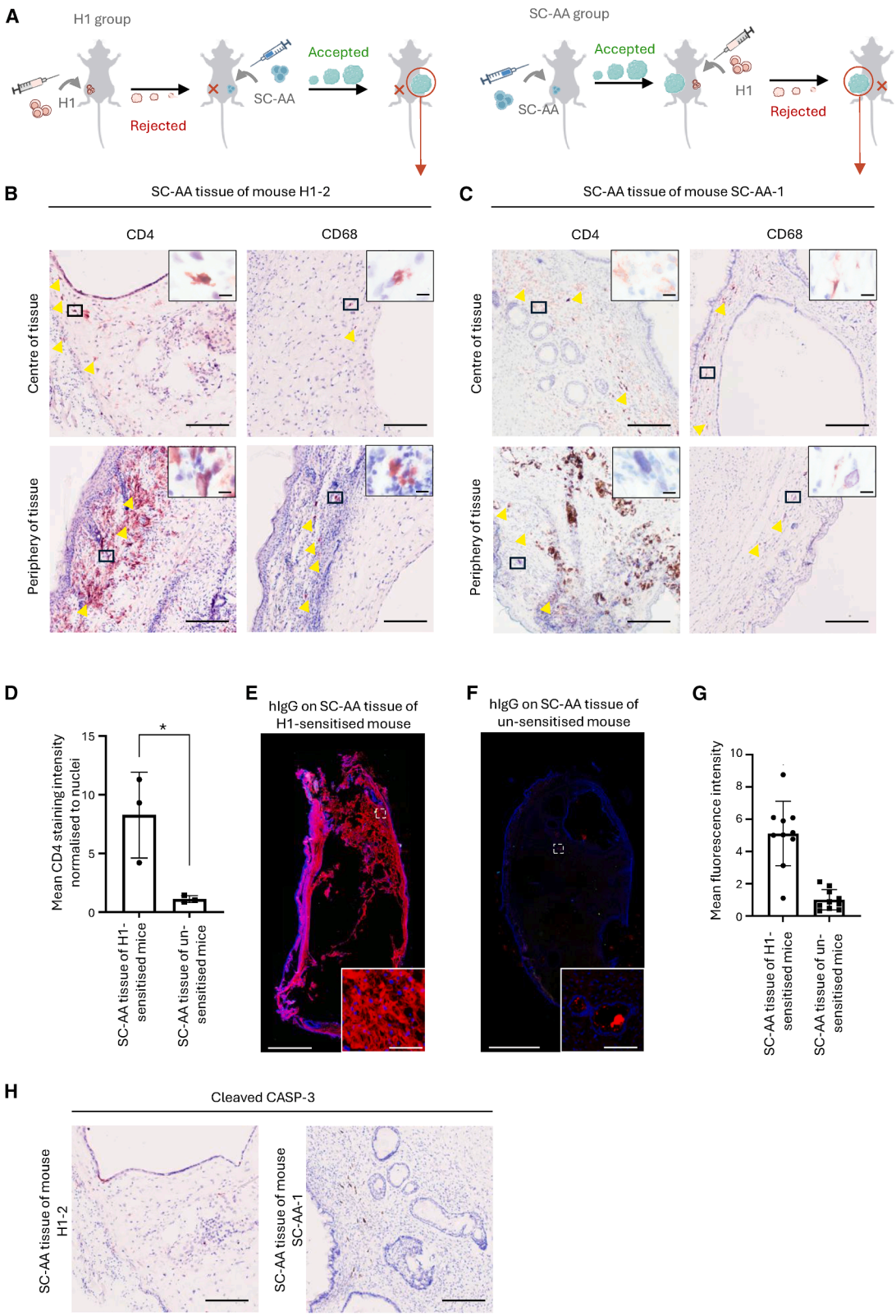

(legend on next page)

Please cite this article in press as: Tam et al., Genome-edited safe and immune-evasive human pluripotent cells: Potential solution for allogeneic therapies, Stem Cell Reports (2026), https://doi.org/10.1016/j.stemcr.2026.102850

DISCUSSION

Allogeneic human PSCs offer abundant functional cell types for replacement therapies, but successful engraftment requires HLA compatibility. Otherwise, patients need systemic immunosuppression, which carries clinical risks, including nephrotoxicity and opportunistic infections, to prevent graft rejection. Several countries are establishing banks of HLA homozygous induced PSC (iPSC) lines to supply immune-matched tissues for allogeneic cell therapies (Alowaysi et al., 2023; Kuebler et al., 2023; Nakatsuji et al., 2008). Even with common HLA haplotypes, large cell banks are needed for reasonable population coverage. Genome-edited immune-evasive pluripotent cells could offer a universal source, potentially eliminating hazardous immunosuppression for allogeneic transplants in many patients across diverse diseases (Harding et al., 2024; Hotta et al., 2024). However, transplanting immune-evasive cells raises safety concerns that bypass the critical immune surveillance system needed eliminate potentially tumorigenic cells. Thus, incorporating a reliable, inducible genetic kill-switch, specifically designed to target rogue cells, is essential (Harding et al., 2020; Liang et al., 2018).

We previously developed safety (SC; Liang et al., 2018) and immune-evasion (AlloAccept; Harding et al., 2024) genome-engineering solutions and generated corresponding genome-edited mouse and human ESCs. Mouse SC-AlloAccept cells met expectation *in vivo*, demonstrating safety and long-term allogeneic acceptance of tissue grafts (Harding et al., 2024; Sawula et al., 2023). Similarly, SC-AlloAccept human ESCs were characterized through *in vitro* interaction with human immune cells (Harding et al., 2024), and by brain transplants in a humanized immune system mouse model of Parkinson's disease (Pavan et al., 2025). However, this model is constrained by the brain's low immunological activity and immune-privileged status. Unlike brain, skin is highly immunologically active, forming a frontline barrier via its structure and resident immune cells. When subcutaneously transplanted, SC-AlloAccept cells engrafted and formed growing tissues in allogeneic humanized immune system mice, unlike wild-type parental human H1 ESCs.

The combination of eight immunomodulatory genes successfully protected the tissue, enabling engraftment and growth of allogeneic human tissue, consistent with previous mouse model predictions (Harding et al., 2024). GCV, the prodrug of the SC kill switch, effectively halted tissue growth, as previously observed in immunocompromised mice (Liang et al., 2018). SafeCell limits excessive proliferation by allowing selective elimination of overgrowing or tumorigenic cells with ganciclovir (Liang et al., 2018). Since *in vitro* grown therapeutic cells can have unintended consequences beyond tumorigenicity, rigorous preclinical testing is required. If necessary for regulatory approval, genomic integration sites can be mapped with a single NGS run (Harding et al., 2024). Furthermore, our platform incorporates a safety switch to mitigate risks from integration effects, disrupted genes, and off-target edits by eliminating proliferating SC-AlloAccept cells regardless of cause. Linking HSV-TK to CDK-1 restricts its expression to dividing cells, avoiding immunogenicity in quiescent cells (Liang et al., 2018). Notably, SC-AlloAccept tissues composed of dividing, HSV-TK-expressing cells were still protected across HLA barriers. GCV-stabilized, dormant SC-AlloAccept tissue persisted for the 5 months *in vivo*, and single-cell transcriptomics provided lineage-level functional insights in this humanized mouse model.

In vitro co-cultures with HLA-mismatched T cells from PBMC showed reduced T cell responses (Harding et al., 2024; Pavan et al., 2025). This attenuation is likely mediated by PD-L1-expressing AlloAccept cells, which engage PD-1 on activated T cells, inducing exhaustion or apoptosis (Gibbons Johnson and Dong, 2017), and by FasL-expressing cells killing Fas (CD95) positive T cells via activation-induced cell death (AICD) (Dhein et al., 1995). *In vivo*, macrophages

Figure 5. Immunohistochemistry analysis of SC-AlloAccept tissue in humanized mice

(A) Schematic of SC-AlloAccept (SC-AA) tissue in H1-2 and SC-AA-1 mice.

(B) IHC for CD4 and CD68 in SC-AA tissue and its periphery of mouse H1-2 (red staining). Area of the high magnification images were indicated with solid line boxes. Scale bars, 200 μm; inset 60x scale bars, 10 μm.

(C) IHC for CD4 and CD68 in SC-AA tissue and its periphery of mouse SC-AA-1 (red staining). Area of the high magnification images were indicated with solid line boxes. Scale bars, 200 μm; inset 60x scale bars, 10 μm.

(D) Mean CD4 staining intensity normalized to nuclei ($n = 3$ biological replicates) showed higher proportions of $CD4^+$ cells in SC-AA tissue of H1-sensitized mice vs. unsensitized mice. Statistical signficance: $*p < 0.05$.

(E) IF staining for human IgG in SC-AA tissue in H1-sensitized mouse H1-2. Scale bars, 1 mm (low magnification) and 50 μm (inset high magnification).

(F) IF staining for human IgG in SC-AA tissue in unsensitized mouse SC-AA-1. Scale bars, 1 mm (low magnification) and 50 μm (inset high magnification).

(G) Higher mean fluorescence intensity in SC-AA tissue of H1-sensitized mice indicated increased human IgG levels compared to unsensitized mice ($n = 10$ technical replicates).

(H) IHC for cleaved CASP-3 in tissues from mice H1-2 and SC-AA-1 (red staining). Scale bars, 200 μm. Yellow arrowheads show representative cells with positive IHC signal.

and T cells were the predominant cell types within allogeneic SC-AlloAccept grafts, but they showed low *IL-12A* and *IFN-γ* expression, and the $CD8^+$ T cells were either inactivated or only moderately activated, suggesting extravasation without activation or cell death. By contrast, mast cells appeared activated. Mast cells promote inflammatory and allograft rejection, yet also contribute to immune tolerance via interactions with Tregs and secreted factors (Elieh Ali Komi and Ribatti, 2019; Nakano et al., 2012).

In autoimmune diseases, the immune system mistakenly attacks self-tissues, destroying specific cell types involved in the disease, via antibody- and T cell-mediated mechanisms. For cell replacement in antibody-mediated autoimmune diseases, such as systemic lupus (Suurmond and Diamond, 2015) and myasthenia gravis (Aarli et al., 1975), preexisting antibodies may threaten allografts. We tested this by first allowing humanized immune system mice to reject parental H1 human ESCs, thereby sensitizing their immune system, and then transplanting SC-AlloAccept cells as a "time-shifted second" graft. Despite the presence of anti-human antibodies, SC-AlloAccept cells engrafted and grew. Lack of cleaved caspase-3 indicated minimal apoptosis, suggesting little or no effective memory response against these cells, or there was a very weak or ineffective memory response against SC-AA cells. Although dissecting the mechanism of memory responses is beyond the scope of this study, our data indicate that the AlloAccept system provides strong protection even in recipients previously sensitized by rejection of parental H1 cells.

The AlloAccept system was designed to act locally (Harding et al., 2024), so system immunosuppression was not expected. Experimentally, we confirmed preserved immunity "time-shifted secondary" transplants of wild-type H1 cells were rejected by the SC-AlloAccept tissue-bearing mice, demonstrating that their systemic immune function remained intact throughout the experimental period. Early B cell dominance in our humanized mice align with reports that B cell proportions are higher from 8 weeks post engraftment of hematopoietic stem and progenitor cells in multiple humanized mouse models (reviewed by Chuprin et al., 2023). B cells, which mature without thymic education, emerge early but remain functionally immature, with full humoral competence depending on subsequent T cell expansion (Yu et al., 2017), which typically becomes significant 15–20 weeks after transplantation (Mian et al., 2020). Humoral immunity, especially donor-specific antibodies, is central to chronic rejection, such as in xenograft heart transplantation failure (Griffith et al., 2025); though cellular immune responses also contribute and cooperate in graft injury and failure (Thaunat, 2012). In our model, early B cell bias declined over time, while human T cells increased.

Our finding that AlloAccept protects human cells aligns with mouse studies showing that the functional orthologues of the immune modulator genes used protect C57BL/6 and FVB cells in multiple inbred and CD1 outbred recipients (Harding et al., 2024). *In vitro* assays using PBMCs of different HLA types similarly showed consistent modulation of PBMC composition and induction of an anti-inflammatory environment during co-culture with SC-AlloAccept cells (Harding et al., 2024; Pavan et al., 2025). Lastly, SafeCell and AlloAccept H1-derived dopaminergic neurons were also protected from rejection in the less immune-active brain of allogeneic humanized mice (Pavan et al., 2025).

Together, our how that the SC-AlloAccept human ESC-derived tissue are stably accepted long-term after subcutaneous implantation into humanized mice bearing an allogeneic immune system, even while parental H1 cells are rejected. The SafeCell system induces dormancy in allogeneic tissues by removing dividing cells, preserving quiescent cells, allowing complex grafts to persist across HLA mismatches without immunosuppression. This supports the potential application of off-the-shelf therapeutic cells generated *in vitro* from an SC-AlloAccept "universal" cell source.

METHODS

Ethics

Animal licences were obtained from the Department of Health of Hong Kong. All procedures were approved by the institutional Committee on the Use of Live Animals in Teaching and Research (CULATR; protocol 23-418) and complied with the institution's guidelines. Use of anonymized blood from the Hong Kong Red Cross Blood Transfusion Service for PBMC isolation (UW 23-551) was reviewed and approved by the Institutional Review Board of the University of Hong Kong/Hospital Authority Hong Kong West Cluster (HKU/HA HKW IRB).

Humanized mice

Female humanized mice (strain: huCD34+HSC-NOD/ShiLt JGpt-*Prkdc*^{em26Cd52}*Il2rg*^{em26Cd22}*Rosa26*$^{em1Cin(hCSF2\&IL3\&KITLG)}$/Gpt, strain number T056601) were purchased from GemPharmatech. Mice with ≥25% human $CD45^+$ leukocytes were considered humanized (Figures S2A and S2B, data and information provided by GemPharmatech). Further details of the mice are provided in the supplemental methods.

Cell lines used in the study

The SC-AlloAccept cell line (Harding et al., 2024) was developed in the laboratory of Andras Nagy from the H1 ESC line HA01 (Wi Cell, USA). Jurkat $CD4^+$ (ATCC, TIB-152, USA) and NK92MI (ATCC, MI CRL-2408, USA) cell lines were provided by Dr. Rio Sugimura (The University of Hong Kong).

HLA typing

Peripheral blood was collected from mouse tail veins into pediatric EDTA tubes. SC-AlloAccept cells were harvested from 6-well plates, washed twice with phosphate buffered saline (PBS), trypsinized, and pelleted. All samples were submitted to the Division of Transplantation and Immunogenetics at Queen Mary Hospital, Hong Kong, for HLA typing.

Transfection of H1 cell line with a luciferase plasmid

To enable longitudinal BLI, the SC-AlloAccept cells and H1 cells were transfected with a luciferase plasmid via the piggyBac transposon system. Detailed procedures and primer sequences are provided in the supplemental methods and Table S1, respectively.

In vitro cell differentiation toward mesoderm/mesendoderm lineage

SC-AlloAccept and H1 cells were differentiated toward the mesoderm lineage for up to 5 days (Zhang et al., 2020) or mesendoderm lineage for up to 7 days (Warin et al., 2024) for *in vitro* experiments, or transplantation to humanized mice. Expression of the 8 transgenes was verified by qPCR as previously described (Harding et al., 2024). Details of cell culture and maintenance are provided in the supplemental methods.

In vitro immunogenicity assessment by co-culture of SC-AlloAccept cells with Jurkat T cells and NK-92 MI cells

SC-AlloAccept and H1 cells were differentiated toward the mesoderm (Zhang et al., 2020) and co-cultured with pre-primed Jurkat T cells at a ratio of T cell:mesodermal SC-AlloAccept/H1 cells of 1:2. The non-adherent T cells were collected, and the activation status assessed by measuring expression of the T cell activation marker CD69 (Biolegend, USA, cat#310906) by flow cytometry and compared to controls (anti-CD3/anti-CD28 activated/untreated T cells).

SC-AlloAccept and H1 cells were differentiated toward the mesoderm (adapted from Zhang et al., 2020) for 2 days and co-cultured with the human NK92MI cell line at a ratio of 1:3 NK cells to mesodermal SC-AlloAccept/H1 cells. The RNA from the non-adherent NK cells was extracted and analyzed by qPCR for proinflammatory markers *IFNG*, *TNF* and *GZMB* using the primers listed in Table S2.

Extraction of human PBMCs and co-culture with SC-AlloAccept cells

Anonymized whole blood was obtained from the Hong Kong Red Cross Blood Transfusion Service and the PBMC were isolated by density gradient centrifugation. Mitomycin C-treated PBMC that were pre-primed were then co-cultured with 7 day-differentiated SC-AlloAccept/H1 cells as previously described (Warin et al., 2024) for 3 days. The media was collected and analyzed for expression of IFN-γ and TNF-α by cytokine ELISA. Detailed procedures are provided in the supplemental methods.

Flow cytometry of blood cells from humanized mice

Mouse tail vein peripheral blood or bone marrow was collected at a specified time points to assess the proportions of immune cells with the following antibodies: APC/Fire 750 anti-mouse CD45 antibody (Biolegend, cat# 103154), BV605 anti-human CD45 antibody (Biolegend, cat# 304042), APC anti-human CD3 antibody (Biolegend, cat#3 00312), PE anti-human CD19 antibody (Biolegend, cat# 302208), and PE/Cyanine 7 CD33 antibody (Biolegend, cat# 303434). Detailed procedures are provided in the supplemental methods.

Cell transplantation and monitoring in humanized mice

Humanized mice were subcutaneously injected down the dorsal flank with 1 million mesendoderm SC-AlloAccept/H1 cells in Matrigel (Corning, Cat #354277) in a 100 μL volume. Transplanted cells were monitored by BLI (refer to supplemental methods) and later measured using a digital caliper on the *x*, *y*, and z axes when palpable tissues were formed to calculate tissue volume. When tissues reached 500 mm^3, the SafeCell system was activated by intraperitoneal injections daily, or every second/third day of GCV (Cytovene, Hainan Poly Pharm Co Ltd, China, cat# HK-63370) at a dose of 50 mg/kg in 100 μL PBS for up to 7–14 days or until tissue growth stopped.

Histology and immunohistochemistry

Tissue masses were dissected, fixed, and processed using standard procedures for paraffin and frozen sample embedding before being cut to 5 μm thickness. Slides were rehydrated using standard procedures and then stained for H&E, or the following antibodies: human nuclear antigen (MyBioSource, cat# MBS4382446) to identify human cells, and also for CD4 (Abcam, cat# ab288724), CD8 (Abcam, cat# ab237709), CD56 (Cell Signaling, cat# 99746T), CD68 macrophages (Abcam, cat# ab213363), and cleaved caspase 3 (Cell Signaling Technology cat# 9661S). Detailed procedures are provided in the supplemental methods.

Statistics

t tests were done to determine the significance between two measurements. Mixed model analysis was done to compare three or more measurements, and Dunnett's multiple comparisons test was done following a significant mixed model analysis result. Statistical significance was defined by a p value <0.05. For bar charts, bar height represented the mean, and the error bar represented the standard deviation.

For a box and whiskers plot, the whiskers represented min to max, and the box represented 25th to 75th percentiles with median in the middle. Statistical analyses were done using GraphPad Prism 8.0.1 or the *t* test function in Excel.

Single-cell RNAseq of an SC-AlloAccept engrafted tissue

The tissue was dissected, digested, and prepared for single-cell RNA-seq using the Chromium Next GEM Single Cell 3' Reagent Kit v3.1 and Chromium Next GEM Chip G Single Cell Kit (10X Genomics) at the Center for PanorOmic Sciences at The University of Hong Kong. Detailed experimental methods, data processing steps and analyses are described in the supplemental methods.

RESOURCE AVAILABILITY

Lead contact

Requests for further information and resources should be directed to and will be fulfilled by the lead contact, Danny Chan (chand@hku.hk).

Materials availability

This study did not generate new unique reagents.

Data and code availability

The raw single-cell RNA-seq data generated in this study has been deposited in the NCBI BioProject database under accession number PRJNA1301068 and Gene Expression Omnibus (GEO) database under accession number GSE319407

ACKNOWLEDGMENTS

Part of this work was funded by the RGC European Union - Hong Kong Research and Innovation Cooperation Co-funding Mechanism, Hong Kong SAR, China (E-HKU703/18) to D.C. A.N. received support from CIHR (Foundation Scheme 143231), Breakthrough T1D (3-SRA-2022-1252-S-B), and Medicine by Design (University of Toronto) and Ontario Research Foundation (MRI ORF RE08-064). The transposase plasmid pEF1a-hyPBase was obtained from Prof. Pengtao Liu (The University of Hong Kong).

AUTHOR CONTRIBUTIONS

Conceptualization, D.C. and A.N. with advice from V.T., N.C.M.W., A.C.H.P., M.Z., E.D.J., and J.K.T.; methodology and data curation, V.T., N.C.M.W., A.C.H.P., M.Z., T.M., J.K., and P.C.; project administration, D.C. and A.N.; formal analysis, V.T., N.C.M.W., A.C.H.P., and M.Z.; writing – original draft preparation, V.T., D.C., N.C.M.W., A.C.H.P., and A.N.; review and editing of the manuscript, V.T., D.C., N.C.M.W., A.C.H.P., A.N., and J.K.; supervision, A.N. and D.C. All authors contributed to the interpretation of the data, read and approved the final manuscript.

DECLARATION OF INTERESTS

A.N. is an inventor on the patent application covering the induced Allogeneic Cell Tolerance (iACT Stealth) Technology (WO/2018/227286) and the patent covering the safe-cell (FailSafe) technology (PCT/CA2016/050256). A.N. is a co-founder and shareholder of panCELLa Inc.

SUPPLEMENTAL INFORMATION

Supplemental information can be found online at https://doi.org/10.1016/j.stemcr.2026.102850.

Received: August 25, 2025
Revised: February 4, 2026
Accepted: February 5, 2026

REFERENCES

Aarli, J.A., Mattsson, C., and Heilbronn, E. (1975). Antibodies against nicotinic acetylcholine receptor and skeletal muscle in human and experimental myasthenia gravis. Scand. J. Immunol. *4*, 849–852. https://doi.org/10.1111/j.1365-3083.1975.tb03727.x.

Abraham, R.T., and Weiss, A. (2004). Jurkat T cells and development of the T-cell receptor signalling paradigm. Nat. Rev. Immunol. *4*, 301–308. https://doi.org/10.1038/nri1330.

Alowaysi, M., Lehmann, R., Al-Shehri, M., Baadhaim, M., Alzahrani, H., Aboalola, D., Zia, A., Malibari, D., Daghestani, M., Alghamdi, K., et al. (2023). HLA-based banking of induced pluripotent stem cells in Saudi Arabia. Stem Cell Res. Ther. *14*, 374. https://doi.org/10.1186/s13287-023-03612-0.

Bifari, F., Pacelli, L., and Krampera, M. (2010). Immunological properties of embryonic and adult stem cells. World J. Stem Cells *2*, 50–60. https://doi.org/10.4252/wjsc.v2.i3.50.

Chuprin, J., Buettner, H., Seedhom, M.O., Greiner, D.L., Keck, J.G., Ishikawa, F., Shultz, L.D., and Brehm, M.A. (2023). Humanized mouse models for immuno-oncology research. Nat. Rev. Clin. Oncol. *20*, 192–206. https://doi.org/10.1038/s41571-022-00721-2.

Dhein, J., Walczak, H., Bäumler, C., Debatin, K.M., and Krammer, P.H. (1995). Autocrine T-cell suicide mediated by APO-1/(Fas/CD95). Nature *373*, 438–441. https://doi.org/10.1038/373438a0.

Drukker, M., Katz, G., Urbach, A., Schuldiner, M., Markel, G., Itskovitz-Eldor, J., Reubinoff, B., Mandelboim, O., and Benvenisty, N. (2002). Characterization of the expression of MHC proteins in human embryonic stem cells. Proc. Natl. Acad. Sci. USA *99*, 9864–9869. https://doi.org/10.1073/pnas.142298299.

Elieh Ali Komi, D., and Ribatti, D. (2019). Mast cell-mediated mechanistic pathways in organ transplantation. Eur. J. Pharmacol. *857*, 172458. https://doi.org/10.1016/j.ejphar.2019.172458.

Gibbons Johnson, R.M., and Dong, H. (2017). Functional Expression of Programmed Death-Ligand 1 (B7-H1) by Immune Cells and Tumor Cells. Front. Immunol. *8*, 961. https://doi.org/10.3389/fimmu.2017.00961.

Griffith, B.P., Grazioli, A., Singh, A.K., Tully, A., Galindo, J., Saharia, K.K., Shah, A., Strauss, E.R., Odonkor, P.N., Williams, B., et al. (2025). Transplantation of a genetically modified porcine heart into a live human. Nat. Med. *31*, 589–598. https://doi.org/10.1038/s41591-024-03429-1.

Harding, J., Vintersten-Nagy, K., and Nagy, A. (2020). Universal Stem Cells: Making the Unsafe Safe. Cell Stem Cell *27*, 198–199. https://doi.org/10.1016/j.stem.2020.07.004.

Harding, J., Vintersten-Nagy, K., Yang, H., Tang, J.K., Shutova, M., Jong, E.D., Lee, J.H., Massumi, M., Oussenko, T., Izadifar, Z., et al. (2024). Immune-privileged tissues formed from immunologically cloaked mouse embryonic stem cells survive long term in allogeneic hosts. Nat. Biomed. Eng. *8*, 427–442. https://doi.org/10.1038/s41551-023-01133-y.

Harper, S.J.F., Ali, J.M., Wlodek, E., Negus, M.C., Harper, I.G., Chhabra, M., Qureshi, M.S., Mallik, M., Bolton, E., Bradley, J.A., and Pettigrew, G.J. (2015). CD8 T-cell recognition of acquired alloantigen promotes acute allograft rejection. Proc. Natl. Acad. Sci. USA *112*, 12788–12793. https://doi.org/10.1073/pnas.1513533112.

Hotta, A., Schrepfer, S., and Nagy, A. (2024). Genetically engineered hypoimmunogenic cell therapy. Nat. Rev. Bioeng. *2*, 960–979. https://doi.org/10.1038/s44222-024-00219-9.

Jentsch-Ullrich, K., Koenigsmann, M., Mohren, M., and Franke, A. (2005). Lymphocyte subsets' reference ranges in an age- and gender-balanced population of 100 healthy adults–a monocentric German study. Clin. Immunol. *116*, 192–197. https://doi.org/10.1016/j.clim.2005.03.020.

Kuebler, B., Alvarez-Palomo, B., Aran, B., Castaño, J., Rodriguez, L., Raya, A., Querol Giner, S., and Veiga, A. (2023). Generation of a bank of clinical-grade, HLA-homozygous iPSC lines with high coverage of the Spanish population. Stem Cell Res. Ther. *14*, 366. https://doi.org/10.1186/s13287-023-03576-1.

Liang, Q., Monetti, C., Shutova, M.V., Neely, E.J., Hacibekiroglu, S., Yang, H., Kim, C., Zhang, P., Li, C., Nagy, K., et al. (2018). Linking a cell-division gene and a suicide gene to define and improve cell therapy safety. Nature *563*, 701–704.

Mahdi, B.M. (2019). Introductory Chapter: Concept of Human Leukocyte Antigen (HLA). In Human Leukocyte Antigen (HLA), B.M. Mahdi, ed. (IntechOpen). https://doi.org/10.5772/intechopen.83727.

Ménoret, S., Renart-Depontieu, F., Martin, G., Thiam, K., and Anegon, I. (2024). Efficient generation of human immune system rats using human CD34(+) cells. Stem Cell Rep. *19*, 1255–1263. https://doi.org/10.1016/j.stemcr.2024.07.005.

Mian, S.A., Anjos-Afonso, F., and Bonnet, D. (2020). Advances in Human Immune System Mouse Models for Studying Human Hematopoiesis and Cancer Immunotherapy. Front. Immunol. *11*, 619236. https://doi.org/10.3389/fimmu.2020.619236.

Nakano, T., Lai, C.Y., Goto, S., Hsu, L.W., Kawamoto, S., Ono, K., Chen, K.D., Lin, C.C., Chiu, K.W., Wang, C.C., et al. (2012). Immunological and regenerative aspects of hepatic mast cells in liver allograft rejection and tolerance. PLoS One *7*, e37202. https://doi.org/10.1371/journal.pone.0037202.

Nakatsuji, N., Nakajima, F., and Tokunaga, K. (2008). HLA-haplotype banking and iPS cells. Nat. Biotechnol. *26*, 739–740. https://doi.org/10.1038/nbt0708-739.

Pavan, C., Davidson, K.C., Payne, N., Frausin, S., Hunt, C.P.J., Moriarty, N., Berrocal Rubio, M.Á., Elahi, Z., Quattrocchi, A.T., Abu-Bonsrah, K.D., et al. (2025). A cloaked human stem-cell-derived neural graft capable of functional integration and immune evasion in rodent models. Cell Stem Cell *32*, 710–726.e8. https://doi.org/10.1016/j.stem.2025.03.008.

Qudus, M.S., Tian, M., Sirajuddin, S., Liu, S., Afaq, U., Wali, M., Liu, J., Pan, P., Luo, Z., Zhang, Q., et al. (2023). The roles of critical pro-inflammatory cytokines in the drive of cytokine storm during SARS-CoV-2 infection. J. Med. Virol. *95*, e28751. https://doi.org/10.1002/jmv.28751.

Sawula, E., Miersch, S., Jong, E.D., Li, C., Chou, F.Y., Tang, J.K., Saberianfar, R., Harding, J., Sidhu, S.S., and Nagy, A. (2023). Cell-based passive immunization for protection against SARS-CoV-2 infection. Stem Cell Res. Ther. *14*, 318. https://doi.org/10.1186/s13287-023-03556-5.

Suurmond, J., and Diamond, B. (2015). Autoantibodies in systemic autoimmune diseases: specificity and pathogenicity. J. Clin. Investig. *125*, 2194–2202. https://doi.org/10.1172/JCI78084.

Szabo, S.J., Sullivan, B.M., Peng, S.L., and Glimcher, L.H. (2003). Molecular mechanisms regulating Th1 immune responses. Annu. Rev. Immunol. *21*, 713–758. https://doi.org/10.1146/annurev.immunol.21.120601.140942.

Tam, Y.K., Maki, G., Miyagawa, B., Hennemann, B., Tonn, T., and Klingemann, H.G. (1999). Characterization of genetically altered, interleukin 2-independent natural killer cell lines suitable for adoptive cellular immunotherapy. Hum. Gene Ther. *10*, 1359–1373. https://doi.org/10.1089/10430349950018030.

Thaunat, O. (2012). Humoral immunity in chronic allograft rejection: puzzle pieces come together. Transpl. Immunol. *26*, 101–106. https://doi.org/10.1016/j.trim.2011.11.003.

Tsai, M., Grimbaldeston, M., and Galli, S.J. (2011). Mast cells and immunoregulation/immunomodulation. Adv. Exp. Med. Biol. *716*, 186–211. https://doi.org/10.1007/978-1-4419-9533-9_11.

Warin, J., Vedrenne, N., Tam, V., Zhu, M., Yin, D., Lin, X., Guidoux-D'halluin, B., Humeau, A., Roseiro, L., Paillat, L., et al. (2024). In vitro and in vivo models define a molecular signature reference for human embryonic notochordal cells. iScience *27*, 109018. https://doi.org/10.1016/j.isci.2024.109018.

Yahata, T., Ando, K., Nakamura, Y., Ueyama, Y., Shimamura, K., Tamaoki, N., Kato, S., and Hotta, T. (2002). Functional human T lymphocyte development from cord blood CD34+ cells in nonobese diabetic/Shi-scid, IL-2 receptor gamma null mice. J. Immunol. *169*, 204–209. https://doi.org/10.4049/jimmunol.169.1.204.

Yu, C.I., Maser, R., Marches, F., Banchereau, J., and Palucka, K. (2024). Protocol to construct humanized mice with adult CD34(+) hematopoietic stem and progenitor cells. STAR Protoc. *5*, 103155. https://doi.org/10.1016/j.xpro.2024.103155.

Yu, H., Borsotti, C., Schickel, J.N., Zhu, S., Strowig, T., Eynon, E.E., Frleta, D., Gurer, C., Murphy, A.J., Yancopoulos, G.D., et al. (2017). A novel humanized mouse model with significant improvement of class-switched, antigen-specific antibody production. Blood *129*, 959–969. https://doi.org/10.1182/blood-2016-04-709584.

Zhang, Y., Zhang, Z., Chen, P., Ma, C.Y., Li, C., Au, T.Y.K., Tam, V., Peng, Y., Wu, R., Cheung, K.M.C., et al. (2020). Directed Differentiation of Notochord-like and Nucleus Pulposus-like Cells Using Human Pluripotent Stem Cells. Cell Rep. *30*, 2791–2806.e5. https://doi.org/10.1016/j.celrep.2020.01.100.